Appendix A.42:

Wharenui School – VsVp 57165

Table 1: Site Description for Wharenui School (VsVp 57165).

Attribute	Yes/No			Description/Date	Symbol in Figure 1
	10-m Buffer	20-m Buffer	50-m Buffer		
Near a body of surface water or other free face features?	No	No	No	The center of the site is ~330 m to the NE from the unnamed pond (the free-face height is ~1.5 m).	NA
Lateral spreading observed during the CES?	No	No	No	No lateral spreading was observed by the mapping team.[1]	NA
Nearby buildings or structures?	No	Yes	Yes	Building coverage of the 20- and 50-m buffers is 15 and 22%, respectively. Buildings are in the NE, NW, and SW quadrants of the 20- and 50-m buffers.	White Fill + Brown Outline
Sloping land?	No	No	No	Flat land, open + residential area	NA
Step changes in the ground surface?	No	No	No	NA	NA
Retaining walls?	No	No	No	NA	NA
Vegetation?	No	Yes	Yes	Trees and bushes cover 16 and 22% of the 20- and 50-m buffers, respectively. They are in the NW and NE quadrants of the 20-m buffer and all quadrants of the 50-m buffer.	White Fill + Green Outline
Anthropogenic changes to the site between the LiDAR surveys?	No	No	No	The sprots field (all quadrants of all buffers) is subject to land resurfacing.	NA
Other important factors?	No	No	No	NA	NA

Note: Buffer is the area within a circle of a specified radius with CPT investigations done at its center (172.597625°, -43.536096°).

[1] Canterbury Geotechnical Database. (2012). "Observed Ground Crack Locations", Map Layer CGD0400 - 23 July 2012, retrieved July 09, 2018 from https://canterburygeotechnicaldatabase.projectorbit.com/

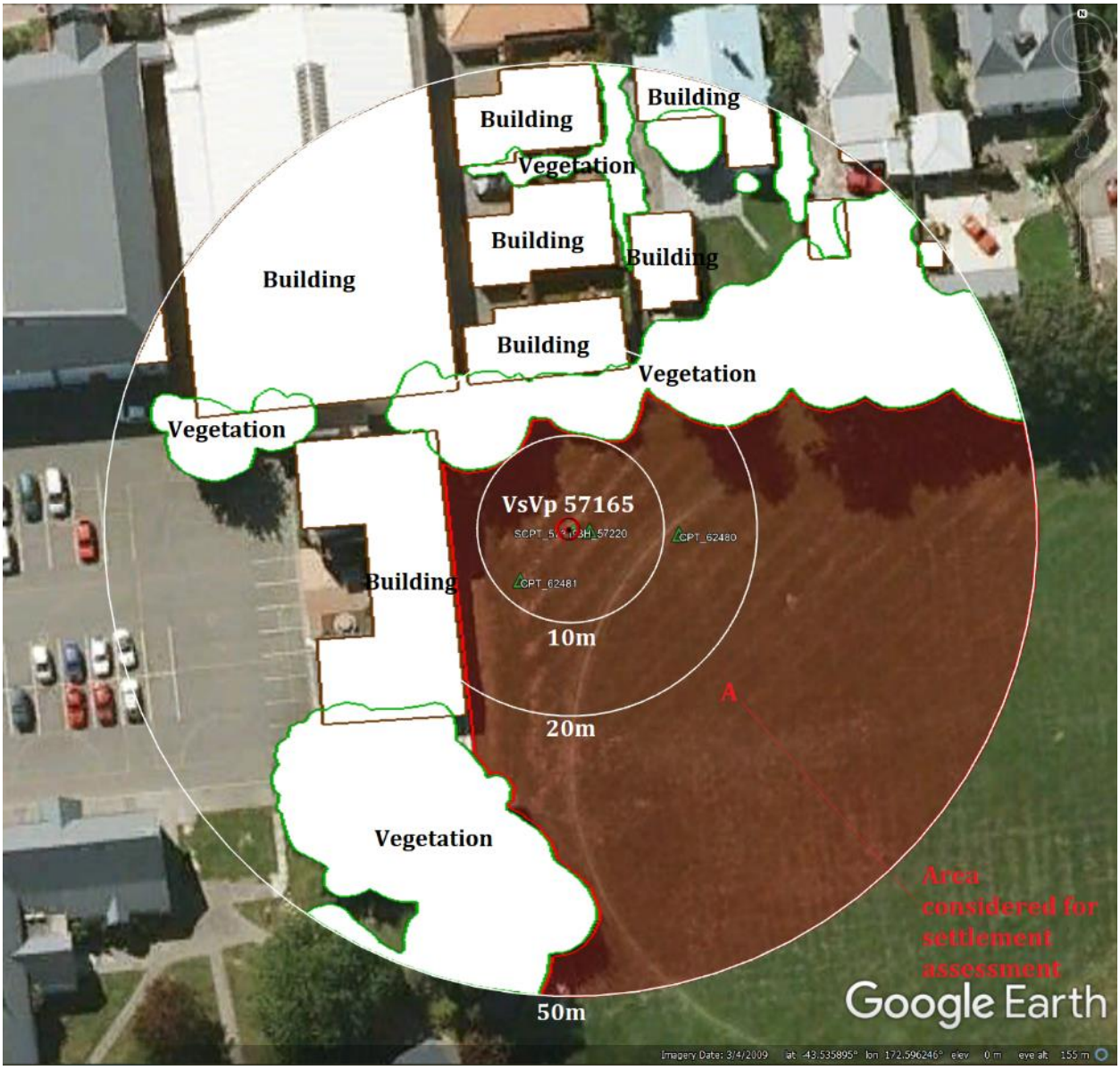

Figure 1: Site plan with areas where ejecta-induced settlement is considered.

Note 1: Patch A (outlined in red) in the free field was selected for settlement assessment as an area free of vegetation and structures. Other important factors considered for the patch selection were its proximity to a CPT, a property subjected to addition and/or demolition of a structure, front yard/backyard alterations (e.g., ploughing, rubble, scrap), and aerial distribution of sediment ejecta. The LiDAR-based settlement analyses were not conducted for any earthquake event due to the evident absence of ejecta from Patch A

Table 2: LiDAR flight error adjustments, global adjustments for the difference between average LiDAR point elevations and benchmark survey elevations, and vertical tectonic movement adjustments.

	Adjustments (mm)		
Earthquake Event(s)	LiDAR Flight Error	Global Offset[2]	Tectonic Vertical Movement
Sep-10	NA	-3	0
Feb-11	NA	16	-50
Jun-11	0	38	-20
Dec-11	NA	-65	0
CES	NA	-14	-70
Any LiDAR survey affected by ejecta?			No

Note: The negative sign indicates the subtraction from the ground surface subsidence, while the positive sign indicates the addition to the ground surface subsidence.

Table 3: LiDAR Measurement Error for Patch A.

Surveys	Buffer	Area Averaged Difference Indicating Repeat Measurement Error (mm)	$\sigma^*_{\text{individual LiDAR points}}$ (mm)	%Reduction in σ due to Area Averaging of LiDAR Points
Post Feb 2011: Mar 2011 and May 2011	10-m	ND	59	[ND,ND]
	20-m	ND		
	50-m	ND		
Post Dec 2011: Feb 2012 and Oct 2015	10-m	NA	70	[NA,NA]
	20-m	NA		
	50-m	NA		

*Standard deviation; NA = Not available; ND = Not determined.

[2] Russell, J., & van Ballegooy, S. (2015). *Canterbury Earthquake Sequence: Increased liquefaction vulnerability assessment methodology*. New Zealand: Tonkin & Taylor Ltd.

Table 4: Ground surface subsidence adjustments due to LiDAR measurement error for Patch A.

Earthquake Event(s)	$\sigma_{\text{pre-EQ LiDAR survey}}$ (mm)	$\sigma_{\text{post-EQ LiDAR survey}}$ (mm)	σ_{total} (mm)	Area Average Adjusted σ (mm) **
Sep-10	158	56	134	±ND
Feb-11	56	59	59	±ND
Jun-11	59	61	62	±ND
Dec-11	61	70	87	±ND
CES	158	70	124	±ND

**Based on the highest %Reduction in Table 3a.

Table 5: Raw liquefaction-related ground surface subsidence using original LiDAR points for Patch A.

	Average Ground Surface Subsidence (mm)		
Earthquake Event(s)	10-m Buffer	20-m Buffer	50-m Buffer
Sep-10	NA	NA	NA
Feb-11	NA	NA	NA
Jun-11	ND	ND	ND
Dec-11	NA	NA	NA
CES	NA	NA	NA

Table 6: Corrected liquefaction-related ground surface subsidence using original LiDAR points for Patch A with the calculated adjustments in Table 2.

	Average Calculated Ground Surface Subsidence (mm)		
Earthquake Event(s)	10-m Buffer	20-m Buffer	50-m Buffer
Sep-10	NA	NA	NA
Feb-11	NA	NA	NA
Jun-11	ND	ND	ND
Dec-11	NA	NA	NA
CES	NA	NA	NA

Notes: Plus/minus values are same as those in Table 4a, but rounded to the nearest 25 mm; Positive overall values indicate ground surface subsidence, while negative overall values indicate ground surface uplift; NA = Not available; ND = Not determined.

Table 7: Corrected liquefaction-related ground surface subsidence for Patch A using LiDAR DEMs.

	Estimated Ground Surface Subsidence (mm)								
	10-m Buffer			20-m Buffer			50-m Buffer		
Earthquake Event(s)	16th %ile	50th %ile	84th %ile	16th %ile	50th %ile	84th %ile	16th %ile	50th %ile	84th %ile
Sep-10	NA	NA	NA	NA	NA	NA	NA	NA	NA
Feb-11	NA	NA	NA	NA	NA	NA	NA	NA	NA
Jun-11	<50	<50	<50	<50	<50	<50	<50	<50	<50
Dec-11	NA	NA	NA	NA	NA	NA	NA	NA	NA
CES	NA	NA	NA	NA	NA	NA	NA	NA	NA

Note: These percentiles are not the exact statistical measures; they indicate the spatial variability of ground surface subsidence.

Table 8a: Ejecta-Induced settlement for the top 20 m of the soil profile for Patch A (10-m buffer) for the 50th %ile PGA, P_L=50%, and C_{FC}=0.13 using BI-2014, ZRB-2002, and I_c cutoff of 2.6.

Earthquake Event(s)	M_W	PGA (g)	Depth to Groundwater (m)	S_T (mm)	S_{V1D} (mm)	$S_{E,L}$ (mm)
Sep-10	7.1	0.22	2.3	NA	70±20	NA
Feb-11	6.2	0.36	2.3	NA	113±50	NA
Jun-11	6.2	0.18	2.3	ND	18±25	ND
Dec-11	6.1	0.17	2.3	NA	11±50	NA

Notes: S_T = Total settlement (Table 6); S_{V1D} = Average vertical settlement due to volumetric compression using Boulanger and Idriss (2014) (BI-2014), Zhang et al. (2002) (ZRB-2002) procedures and de Greef and Lengkeek (2018) thin-layer correction; $S_{E,L}$ = Ejecta-induced settlement as the difference between the LiDAR-based S_T and S_{V1D}.

Table 8b: Ejecta-Induced settlement for the top 20 m of the soil profile for Patch A (20-m buffer) for the 50th %ile PGA, P_L=50%, and C_{FC}=0.13 using BI-2014, ZRB-2002, and I_c cutoff of 2.6.

Earthquake Event(s)	M_W	PGA (g)	Depth to Groundwater (m)	S_T (mm)	S_{V1D} (mm)	$S_{E,L}$ (mm)
Sep-10	7.1	0.22	2.3	NA	74±20	NA
Feb-11	6.2	0.36	2.3	NA	121±50	NA
Jun-11	6.2	0.18	2.3	ND	18±25	ND
Dec-11	6.1	0.17	2.3	NA	11±50	NA

Notes: S_T = Total settlement (Table 6); S_{V1D} = Average vertical settlement due to volumetric compression using Boulanger and Idriss (2014) (BI-2014), Zhang et al. (2002) (ZRB-2002) procedures and de Greef and Lengkeek (2018) thin-layer correction; $S_{E,L}$ = Ejecta-induced settlement as the difference between the LiDAR-based S_T and S_{V1D}.

Table 8c: Ejecta-Induced settlement for the top 20 m of the soil profile for Patch A (50-m buffer) for the 50th %ile PGA, P_L=50%, and C_{FC}=0.13 using BI-2014, ZRB-2002, and I_C cutoff of 2.6.

Earthquake Event(s)	M_W	PGA (g)	Depth to Groundwater (m)	S_T (mm)	S_{V1D} (mm)	$S_{E,L}$ (mm)
Sep-10	7.1	0.22	2.3	NA	80±20	NA
Feb-11	6.2	0.36	2.3	NA	130±50	NA
Jun-11	6.2	0.18	2.3	ND	20±25	ND
Dec-11	6.1	0.17	2.3	NA	12±50	NA

Notes: S_T = Total settlement (Table 6); S_{V1D} = Average vertical settlement due to volumetric compression using Boulanger and Idriss (2014) (BI-2014), Zhang et al. (2002) (ZRB-2002) procedures and de Greef and Lengkeek (2018) thin-layer correction; $S_{E,L}$ = Ejecta-induced settlement as the difference between the LiDAR-based S_T and S_{V1D}.

Note 2: The uncertainty for volumetric settlement was derived based on the sensitivity of volumetric settlement to PGA, C_{FC}, and P_L for each earthquake event for VsVp 57203 *Shirley Intermediate School* and CC LIQ 1 – CPT 5586 – *Vivian St* sites. Taking the 50th percentile as the baseline case, the minimum and maximum values corresponding to the difference between the 25th percentile and the 50th percentile and the 75th percentile and the 50th percentile were determined. The arithmetic mean of the range of the minimum and maximum difference was evaluated for each patch at the two sites. The maximum arithmetic mean for each earthquake event was rounded to the nearest five and used as the uncertainty value. Accordingly, the 1-D volumetric settlement uncertainties of ±20, ±50, ±25, and ±50 mm for the Sep-10, Feb-11, Jun-11, and Dec-11 earthquake events, respectively, were used for all sites in this study.

Table 9a: Coverage area and height of ejecta estimates for Patch A (10-m buffer) using photographs.

Earthquake Event	$A_{E,thick}$ (m^2)	$H_{E,thick}$ (mm)	$A_{E,thin}$ (m^2)	$H_{E,thin}$ (mm)	A_T (m^2)
Sep-10	0	0	0	0	314
Feb-11	0	0	0	0	314
Jun-11	0	0	0	0	314
Dec-11	0	0	0	0	314

Notes: $A_{E,thick/thin}$ = Coverage area of thick/thin ejecta layers; $H_{E,thick/thin}$ = Lower-upper estimate of height of thick/thin ejecta layers; A_T = Total assessment area of a buffer being considered; Thin and thick layers correspond to light gray and dark gray colors of ejecta observed in aerial photographs.

Table 9b: Coverage area and height of ejecta estimates for Patch A (20-m buffer) using photographs.

Earthquake Event	$A_{E,thick}$ (m^2)	$H_{E,thick}$ (mm)	$A_{E,thin}$ (m^2)	$H_{E,thin}$ (mm)	A_T (m^2)
Sep-10	0	0	0	0	858
Feb-11	0	0	0	0	858
Jun-11	0	0	0	0	858
Dec-11	0	0	0	0	858

Notes: $A_{E,thick/thin}$ = Coverage area of thick/thin ejecta layers; $H_{E,thick/thin}$ = Lower-upper estimate of height of thick/thin ejecta layers; A_T = Total assessment area of a buffer being considered; Thin and thick layers correspond to light gray and dark gray colors of ejecta observed in aerial photographs.

Table 9c: Coverage area and height of ejecta estimates for Patch A (50-m buffer) using photographs.

Earthquake Event	$A_{E,thick}$ (m^2)	$H_{E,thick}$ (mm)	$A_{E,thin}$ (m^2)	$H_{E,thin}$ (mm)	A_T (m^2)
Sep-10	0	0	0	0	2998
Feb-11	0	0	0	0	2998
Jun-11	0	0	0	0	2998
Dec-11	0	0	0	0	2998

Notes: $A_{E,thick/thin}$ = Coverage area of thick/thin ejecta layers; $H_{E,thick/thin}$ = Lower-upper estimate of height of thick/thin ejecta layers; A_T = Total assessment area of a buffer being considered; Thin and thick layers correspond to light gray and dark gray colors of ejecta observed in aerial photographs.

Note 3: The values in Table 9 correspond to the coverage area of ejecta as per aerial photographs and satellite images (Figures 7, 8, 18, 19, and 21) and the lower and upper estimates of ejecta height based on geometrical approximations, ground photographs, and EQC LDAT property inspection reports. The ejecta-induced settlement using photographs and engineering judgment, $S_{E,P}$, is estimated as

$$S_{E,P} = \frac{\sum_{i=1}^{a} A_{E,thick,i} * H_{E,thick,i} + \sum_{j=1}^{b} A_{E,thin,j} * H_{E,thin,j}}{A_T} += \frac{\sum_{i=1}^{a} V_{E,thick,i} + \sum_{j=1}^{b} V_{E,thin,j}}{A_T}$$

where

- $A_{E,thick,i}$ and $H_{E,thick,i}$ are the area and the height of a thick ejecta layer, respectively;
- $A_{E,thin,j}$ and $H_{E,thin,j}$ are the area and the height of a thin ejecta layer, respectively;
- A_T is the total assessment area for a buffer being considered (Figure 1).

Table 10: Ejecta-induced settlement estimates for Patch A based on photographs.

Earthquake Event	Patch A (10-m buffer)		Patch A (20-m buffer)		Patch A (50-m buffer)	
	$S_{E,P,lower}$ (mm)	$S_{E,P,upper}$ (mm)	$S_{E,P,lower}$ (mm)	$S_{E,P,upper}$ (mm)	$S_{E,P,lower}$ (mm)	$S_{E,P,upper}$ (mm)
Sep-10	0	0	0	0	0	0
Feb-11	0	0	0	0	0	0
Jun-11	0	0	0	0	0	0
Dec-11	0	0	0	0	0	0

Note: $S_{E,P,lower}$ and $S_{E,P,upper}$ correspond to lower and upper estimates of $S_{E,P}$, respectively.

Table 11: Best final estimates of ejecta-induced settlement for Patches A, B, and C.

EQ Event	Patch A (10-m buffer)			Patch A (20-m buffer)			Patch A (50-m buffer)		
	$S_{E,L}$ (mm)	$S_{E,P}$ (mm)	$S_{E,final}$ (mm)	$S_{E,L}$ (mm)	$S_{E,P}$ (mm)	$S_{E,final}$ (mm)	$S_{E,L}$ (mm)	$S_{E,P}$ (mm)	$S_{E,final}$ (mm)
Sep-10	NA	0	0	NA	0	0	NA	0	0
Feb-11	NA	0	0	NA	0	0	NA	0	0
Jun-11	ND	0	0	ND	0	0	ND	0	0
Dec-11	NA	0	0	NA	0	0	NA	0	0

Notes: $S_{E,L}$ = Ejecta-induced settlement based on LiDAR data reported in Table 8; $S_{E,P}$ = Median ejecta-induced settlement for the range of values reported in Table 10; $S_{E,final}$ = Best final estimate of ejecta-induced settlement rounded to the nearest 5 mm; Final plus/minus values are also rounded to the nearest 5 mm; NA = Not available; ND = Not determined.

Note 4:

- $S_{E,final}$ for Patch A is based solely on $S_{E,P}$ for all earthquake events due to the evident absence of ejecta.
- The LiDAR-based ground surface subsidence for the Sep-10 and Feb-11 EQ is not available for the Wharenui School site. The LPI prediction error by Maurer et al. (2014[3]) is not available for the site. The LDAT property inspection reports do not exist for the properties within 50-m buffer. There is no visual evidence of ejecta in the aerial photographs.

Summary:

The best estimate of the ejecta-induced free-field ground settlement at the Wharenui School St site for the SEP 2010, FEB 2011, JUN 2011, and DEC 2011 earthquake is 0 mm, 0 mm, 0 mm, and 0 mm, respectively.

[3] Maurer, B. W., Green, R. A., Cubrinovski, M., & Bradley, B. A. (2014). Evaluation of the Liquefaction Potential Index for Assessing Liquefaction Hazard in Christchurch, New Zealand. *Journal of Geotechnical and Geoenvironmental Engineering*, 140(7), 04014032-1-11. doi:10.1061/(asce)gt.1943-5606.0001117

Figure 2: Location of the site.

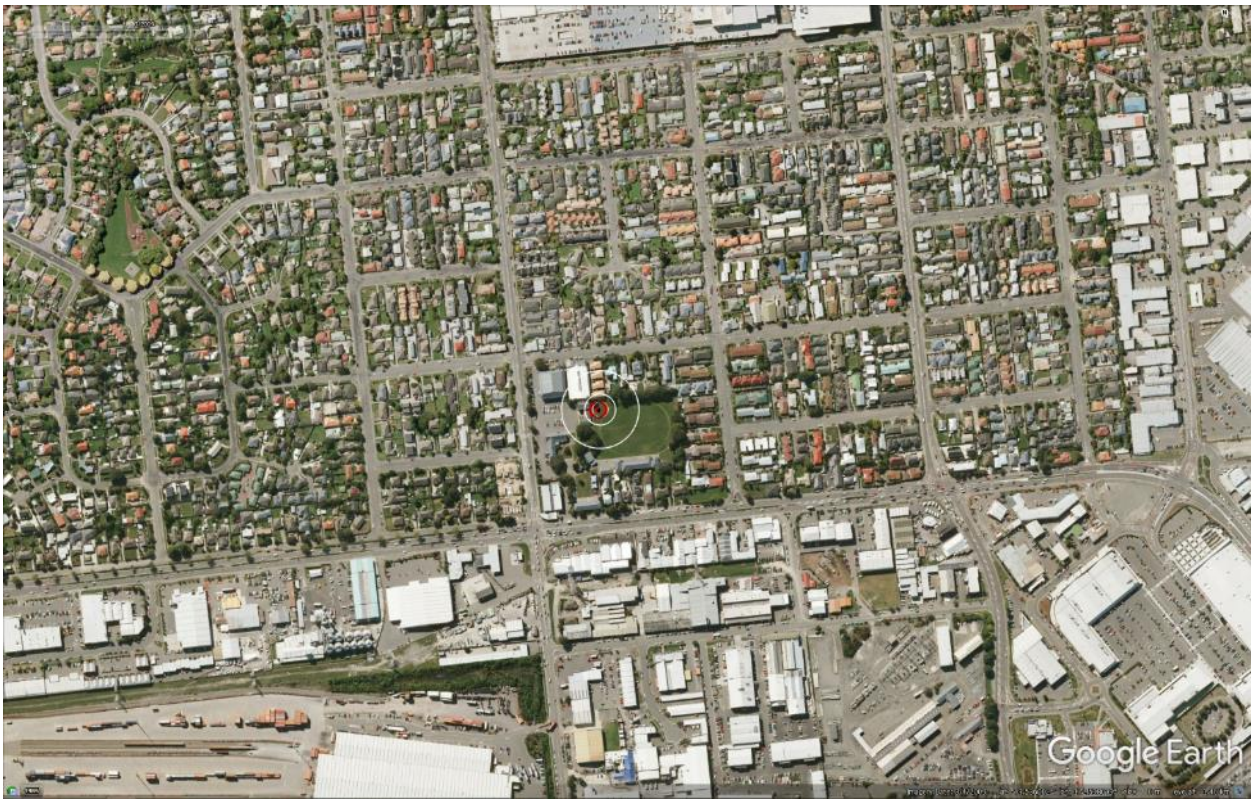

Figure 3: Position of the site relative to nearby buildings, vegetation, and free-face features.

Figure 4: Street view of the flat land.

Figure 5: Satellite image of the site taken in Apr 2004.

Figure 6: Satellite image of the site taken in Mar 2009.

Figure 7: Satellite image of the site taken on Sep 3, 2010.

Figure 8: Satellite image of the site taken on Sep 5, 2010.

Figure 9: Satellite image of the site taken on Feb 15, 2011.

Figure 10: Satellite image of the site taken on Feb 23, 2011.

Figure 11: Satellite image of the site taken on Feb 26, 2011.

Figure 12: Satellite image of the site taken on Mar 28, 2011.

Figure 13: Satellite image of the site taken on Aug 30, 2011.

Figure 14: Satellite image of the site taken in Apr 2012.

Figure 15: Satellite image of the site taken in Nov 2015.

Figure 16: Aerial photograph of the site taken on Sep 4, 2010.

Figure 17: Aerial photograph of the site taken on Feb 24, 2011.

Figure 18: Aerial photograph of the site taken on June 14-15, 2011.

Figure 19: Aerial photograph of the site taken on June 16, 2011.

Figure 20: Aerial photograph of the site taken on Dec 24, 2011.

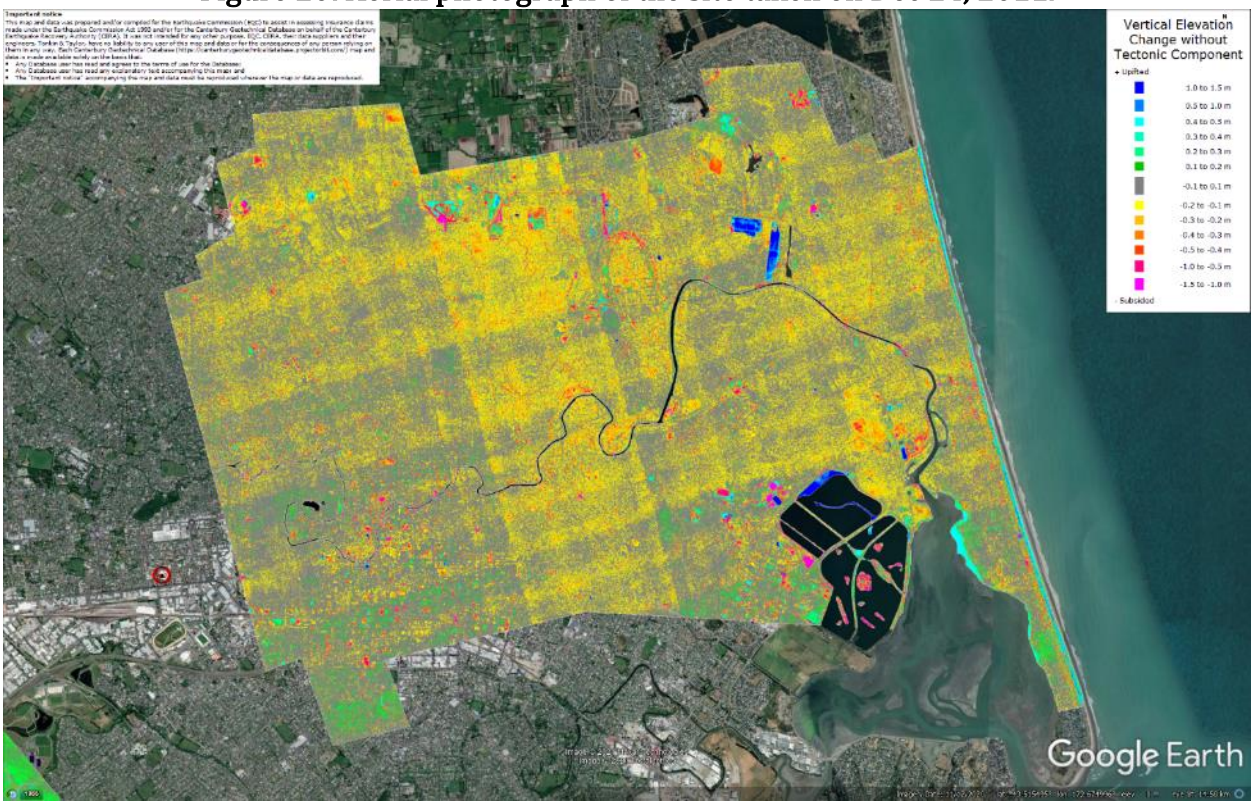

Figure 21: Vertical Ground Movements (Surface – Tectonic) for Sep 2010 Earthquake are not available.

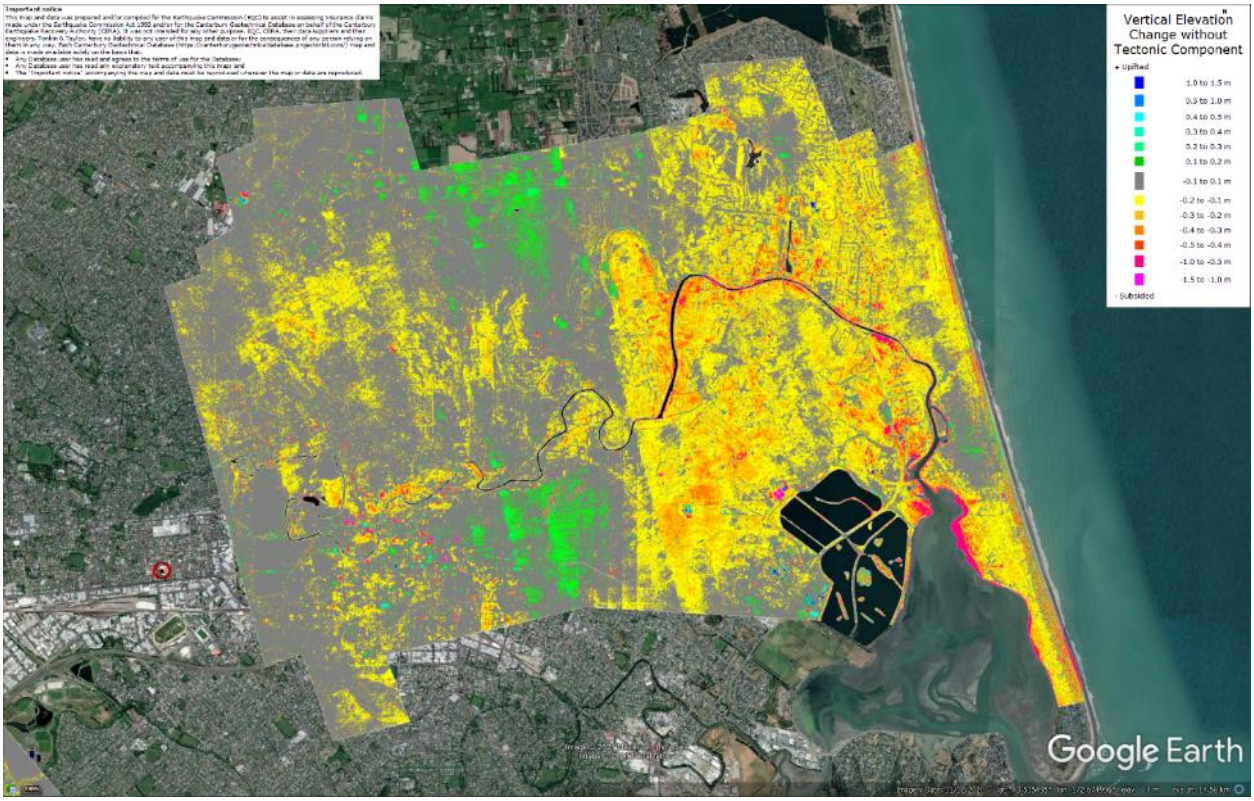

Figure 22: Vertical Ground Movements (Surface – Tectonic) for Feb 2011 Earthquake are not available.

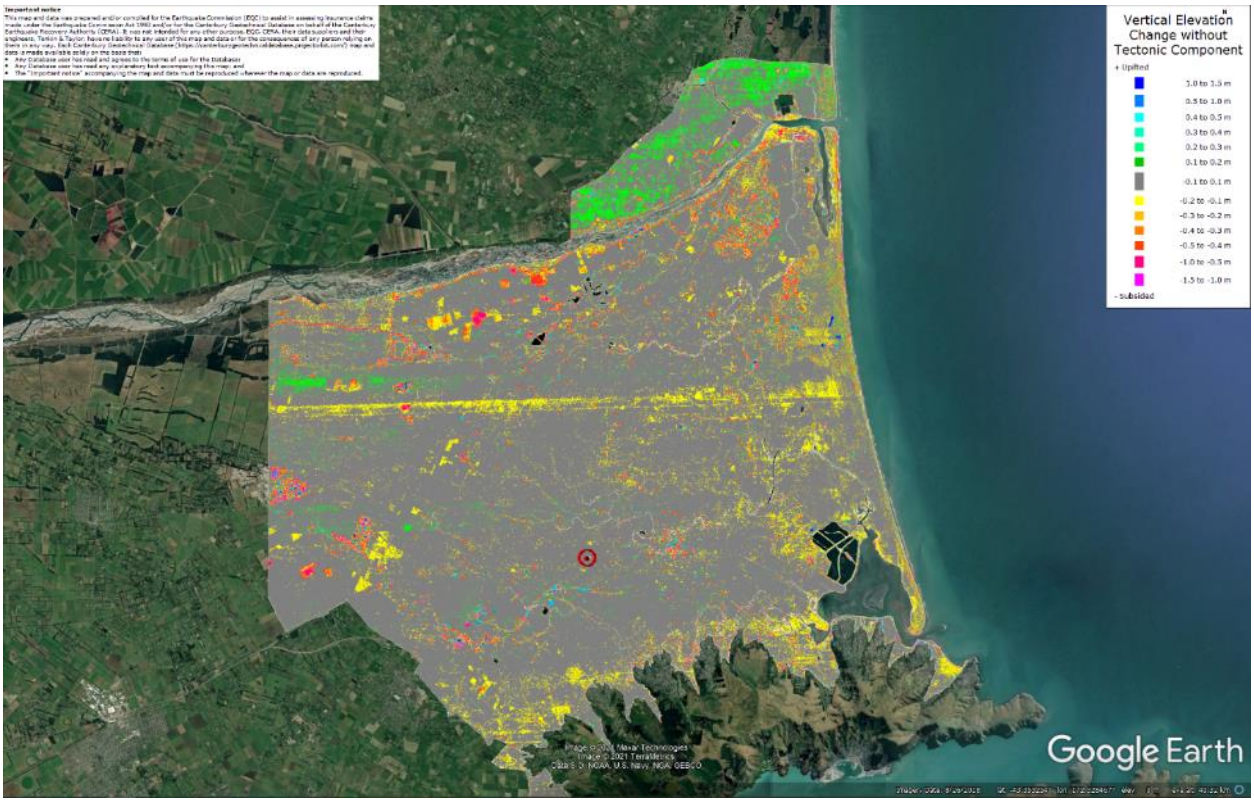

Figure 23: Vertical Ground Movements (Surface – Tectonic) for June 2011 Earthquake – the site is not in the apparent zone of overestimated or underestimated ground surface subsidence.

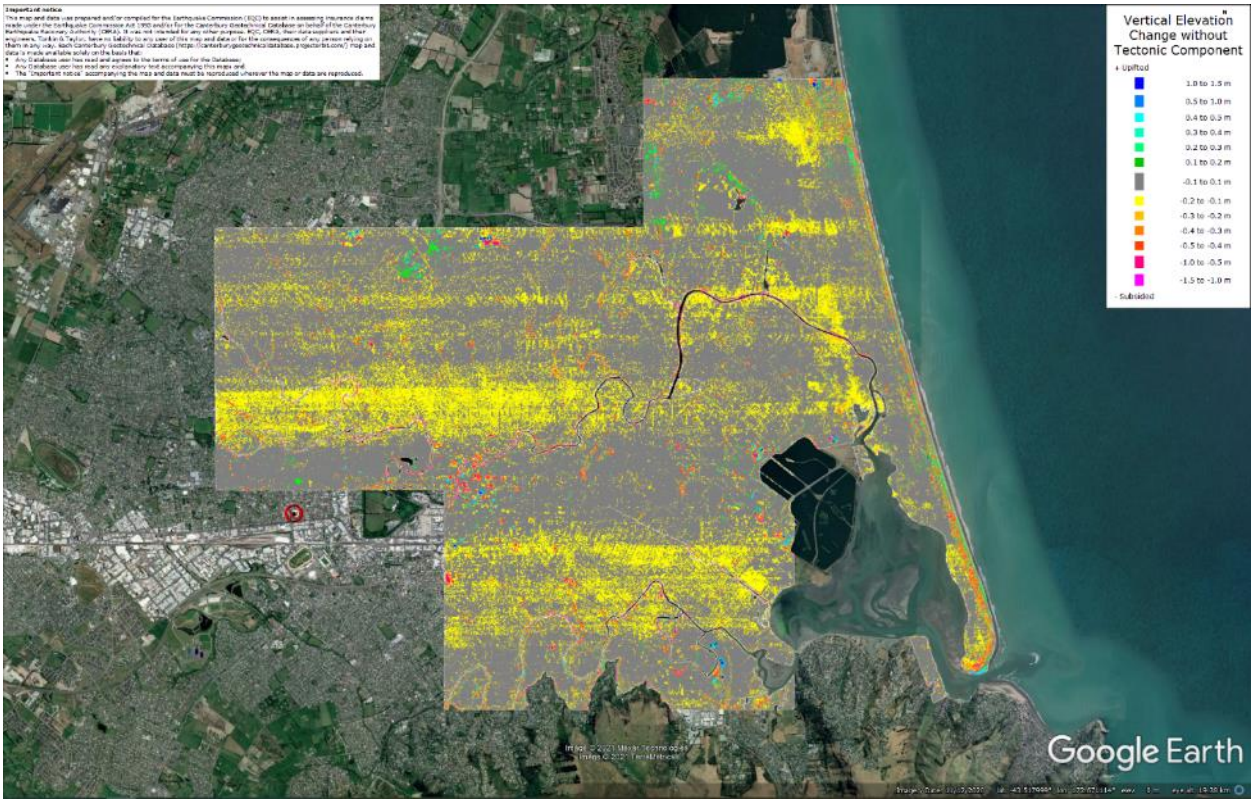

Figure 24: Vertical Ground Movements (Surface – Tectonic) for Dec 2011 Earthquake are not available.

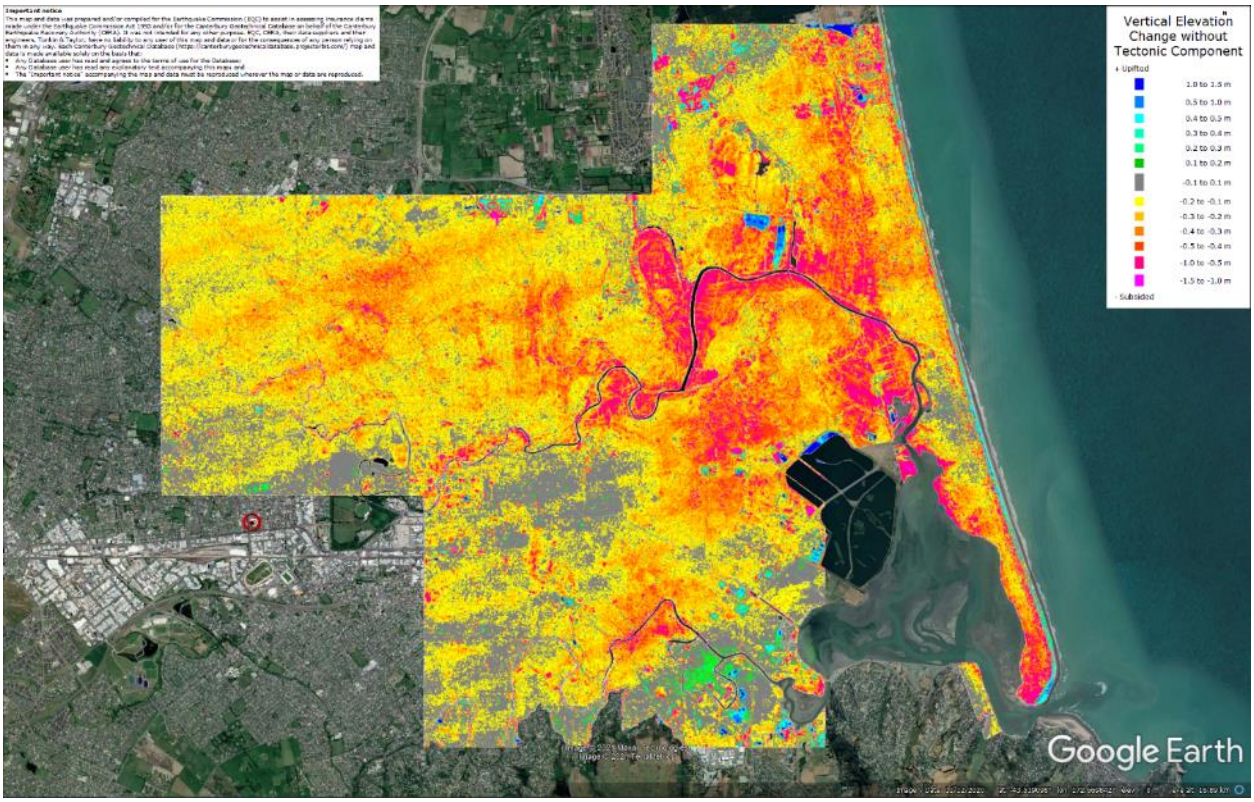

Figure 25: Vertical Ground Movements (Surface – Tectonic) for Canterbury Earthquake Sequence are not available.

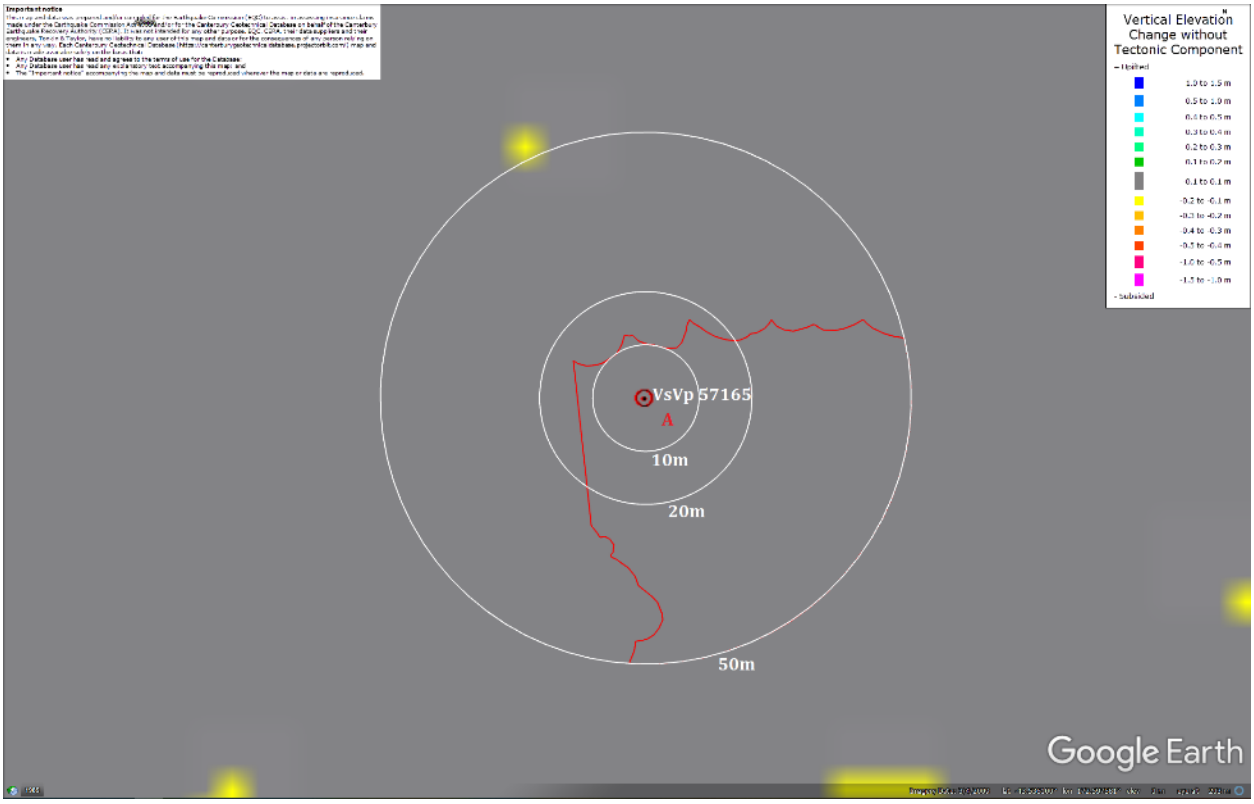

Figure 26: Ground surface subsidence without tectonic component for June 2011 Earthquake according to the LiDAR DEM.

Figure 27: No lateral spreading for Canterbury Earthquake Sequence.

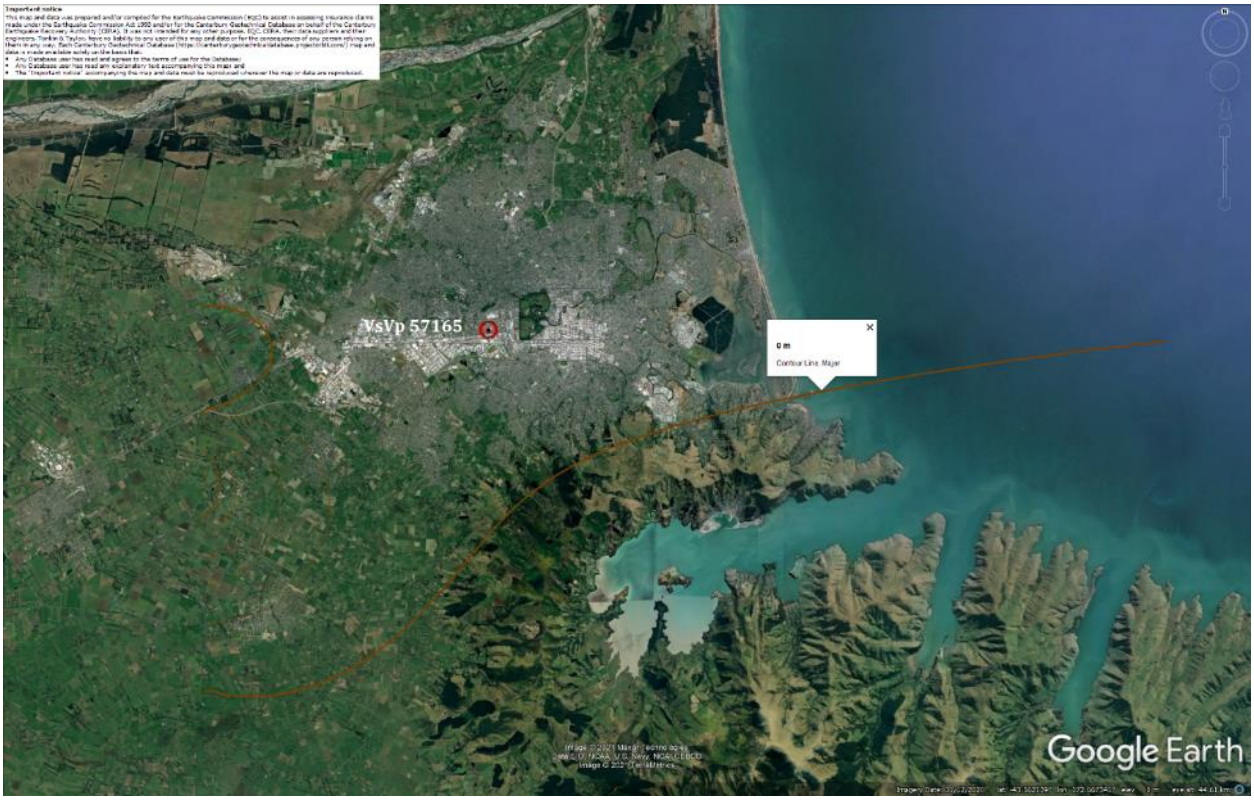

Figure 28: Vertical tectonic movements for Sep 2010 Earthquake.

Figure 29: Vertical tectonic movements for Feb 2011 Earthquake.

Figure 30: Vertical tectonic movements for June 2011 Earthquake.

Figure 31: Vertical tectonic movements for Dec 2011 Earthquake.

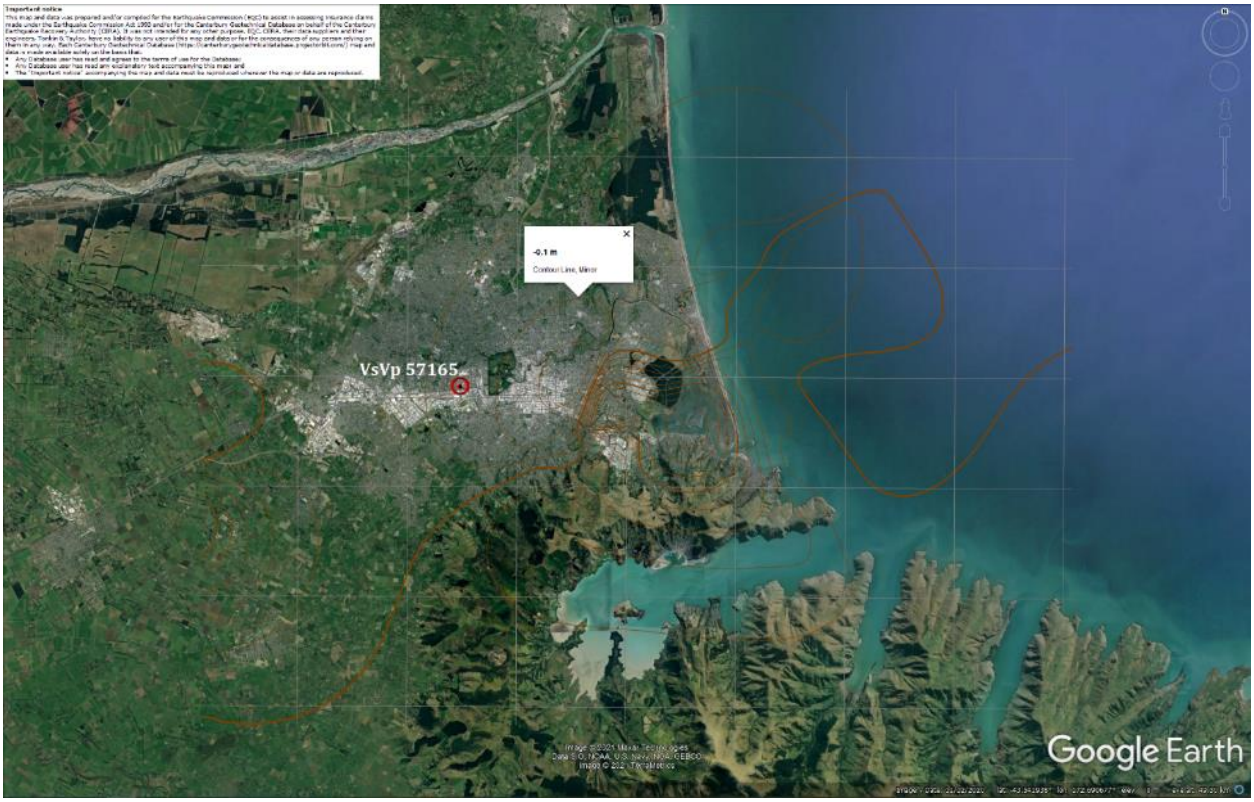

Figure 32: Vertical tectonic movements for Canterbury Earthquake Sequence.

Figure 33: PGA for Sep-10 EQ (st. dev. = 0.325-0.350 ln units).

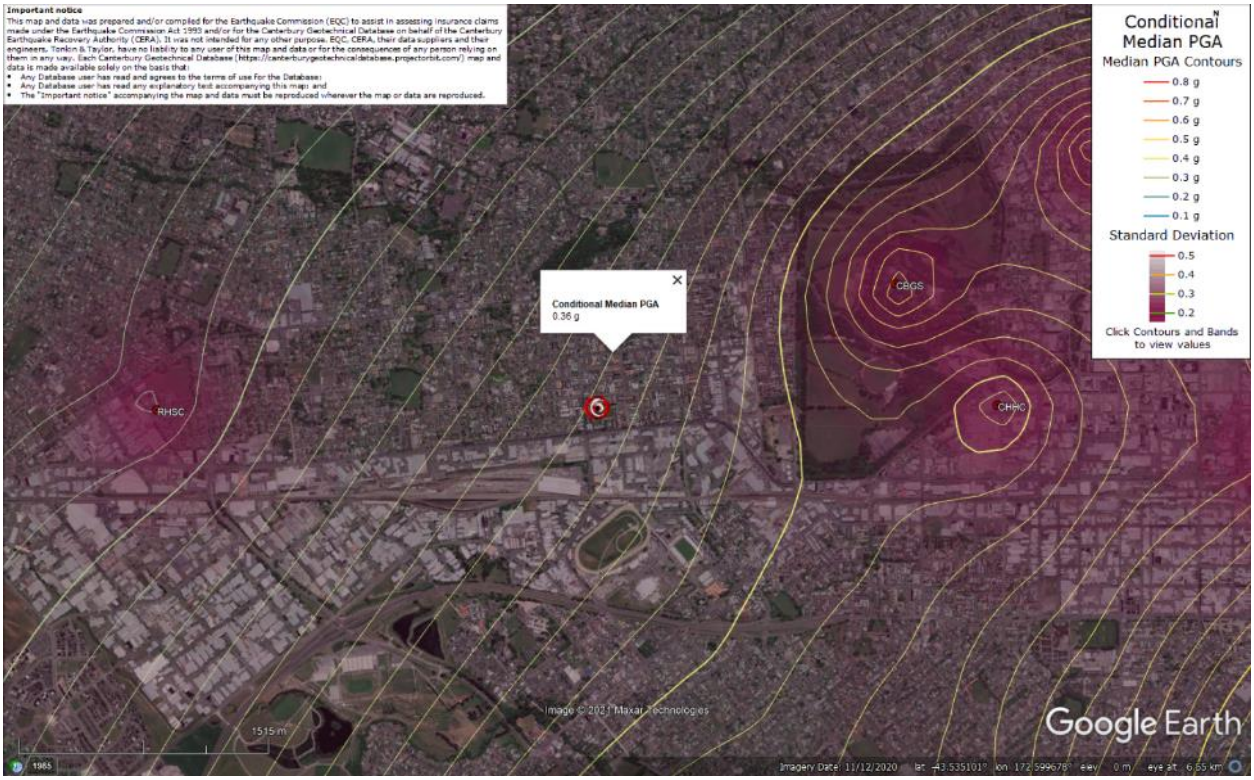

Figure 34: PGA for Feb-11 EQ (st. dev. = 0.350-0.375 ln units).

Figure 35: PGA for Jun-11 EQ (st. dev. = 0.375-0.400 ln units).

Figure 36: PGA for Dec-11 EQ (st. dev. = 0.375-0.400 ln units).

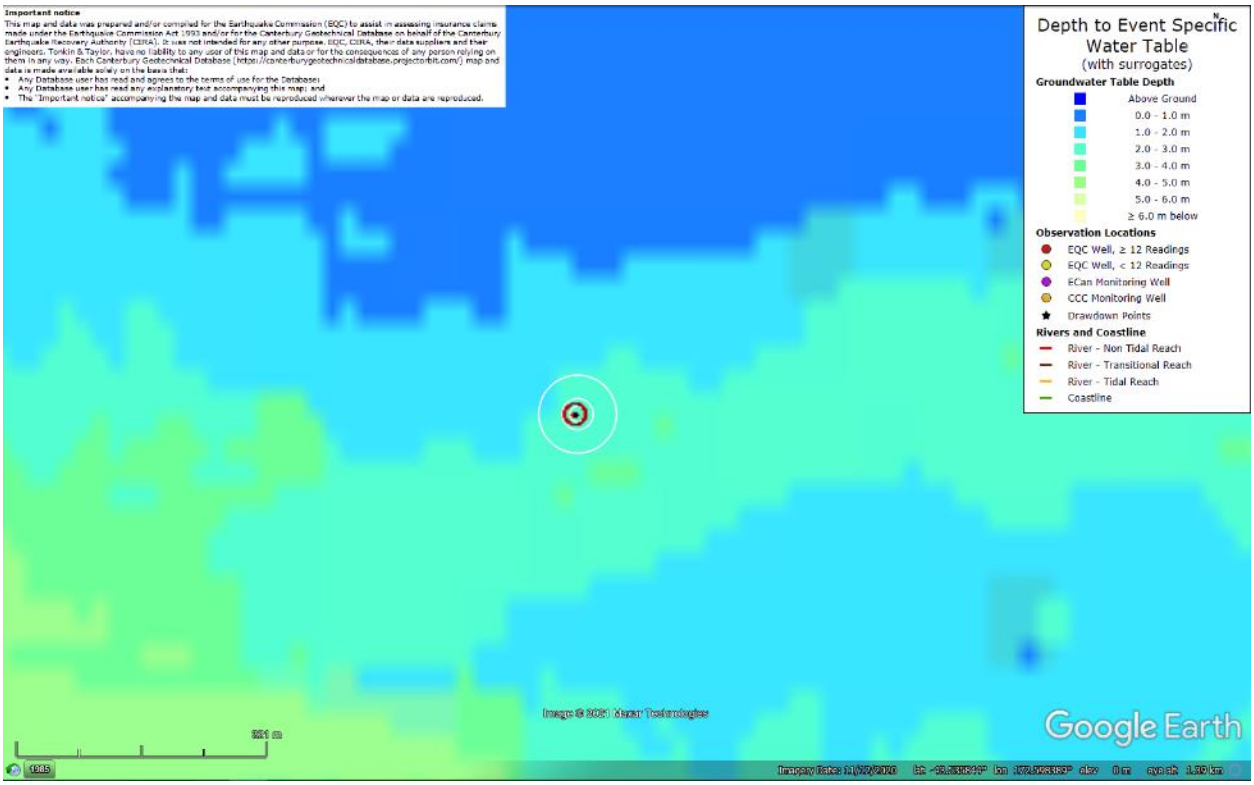

Figure 37: Depth to groundwater table for Sep-10 EQ.

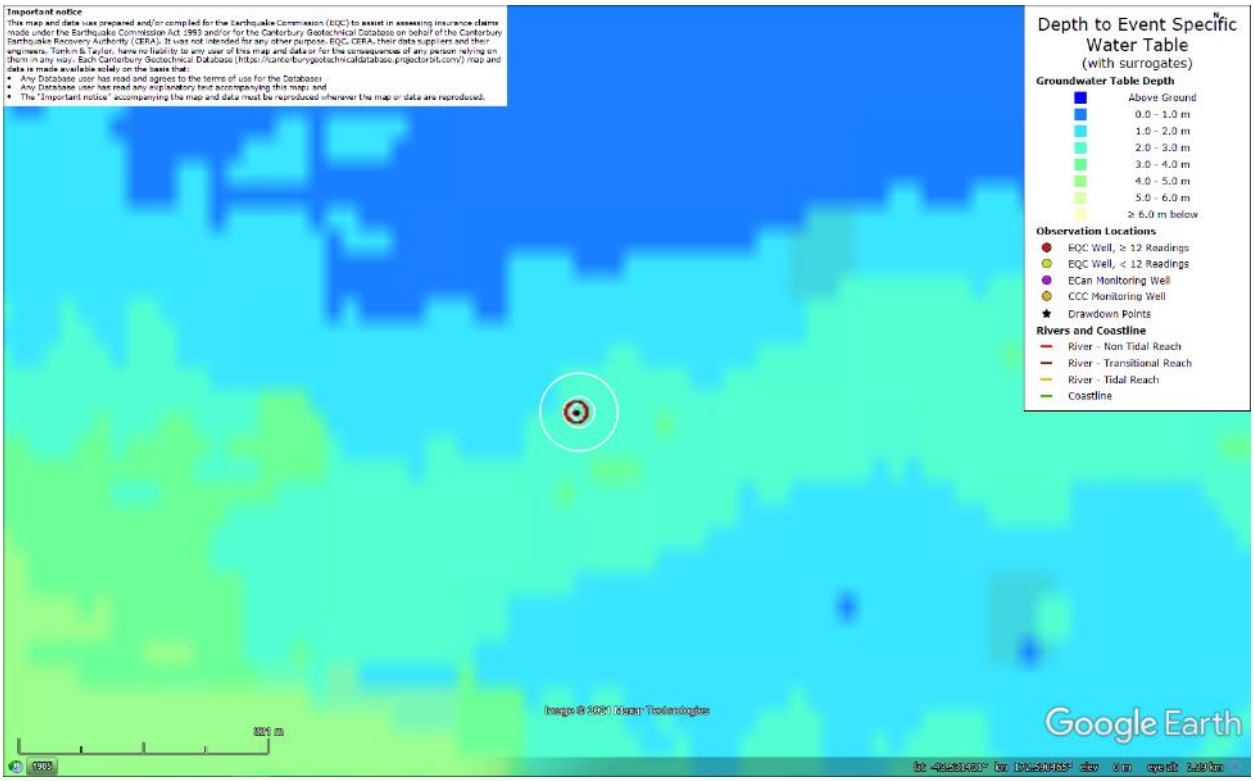

Figure 38: Depth to groundwater table for Feb-11 EQ.

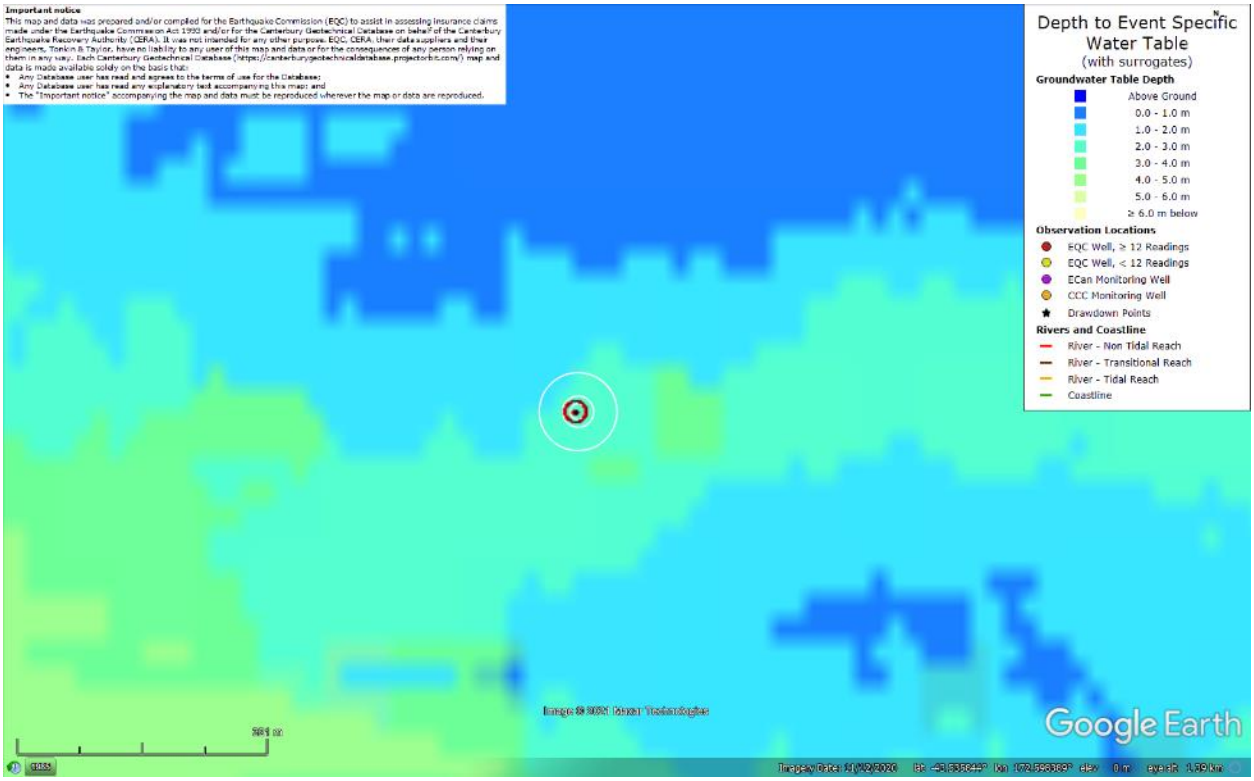

Figure 39: Depth to groundwater table for Jun-11 EQ.

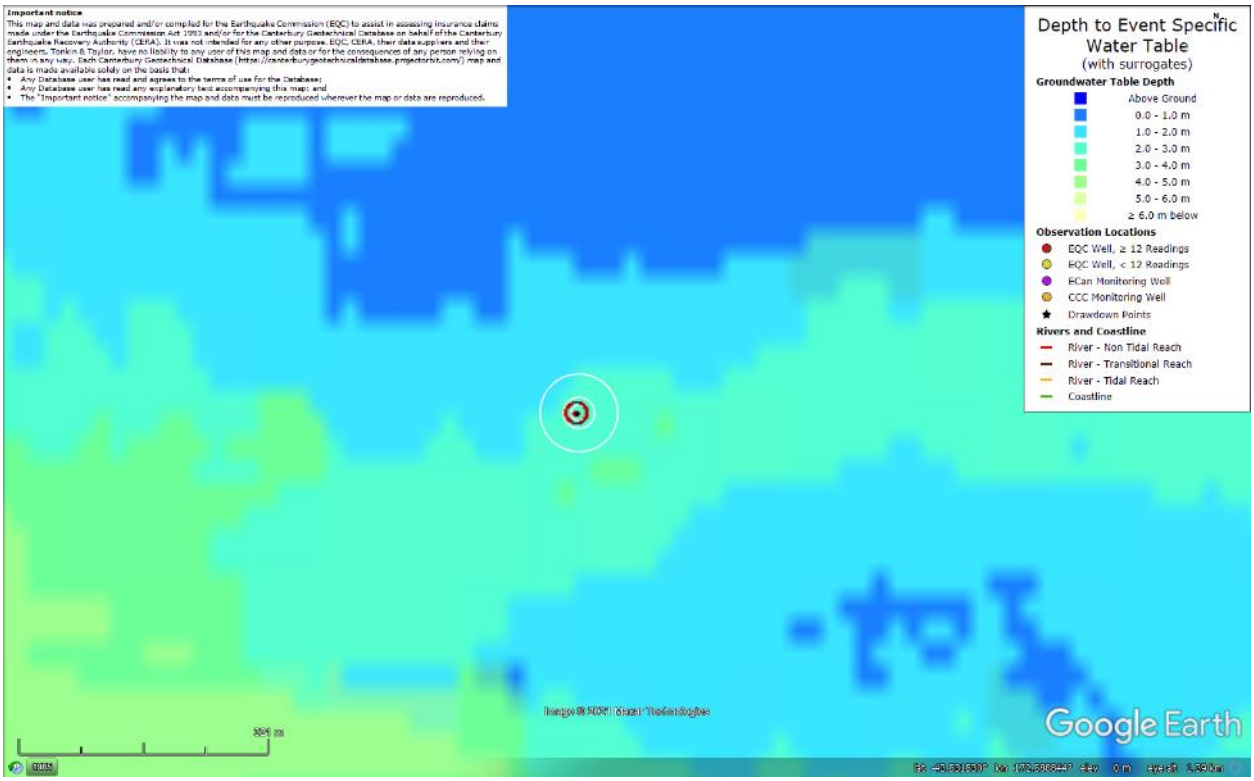

Figure 40: Depth to groundwater table for Dec-11 EQ.

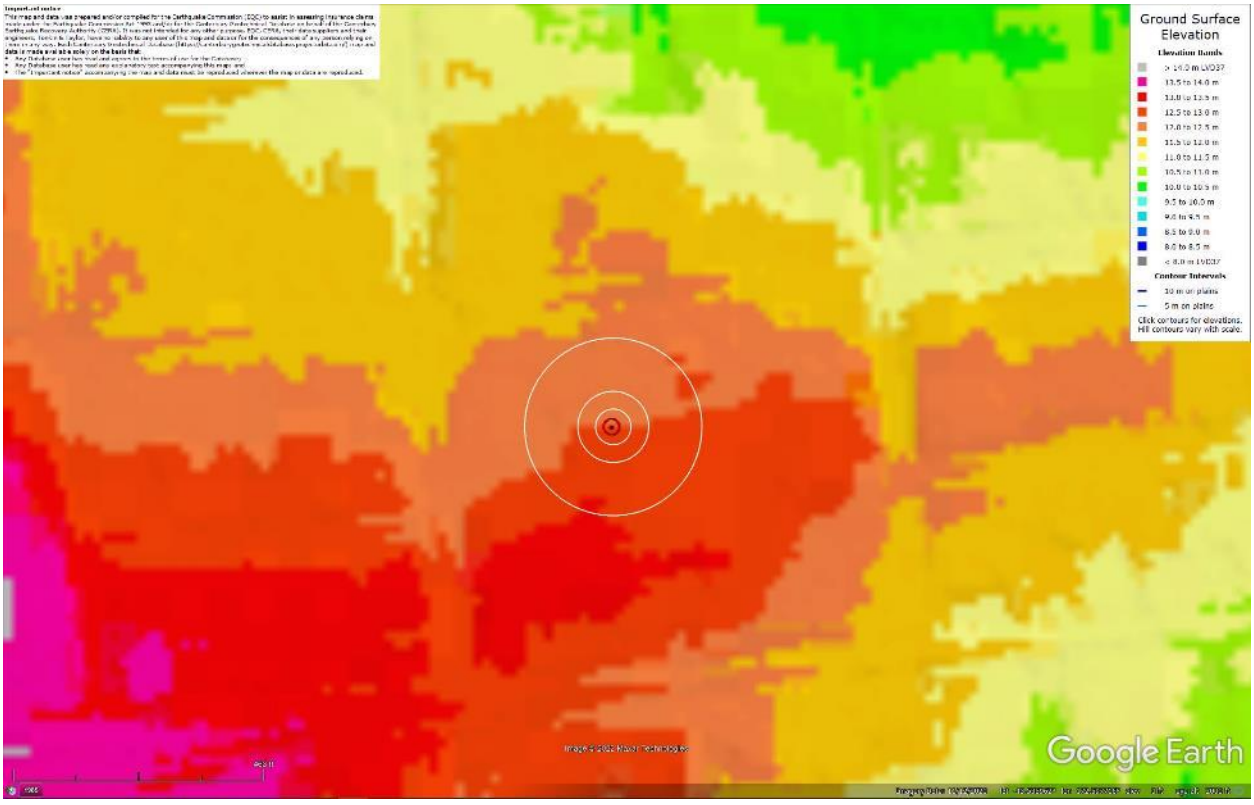

Figure 41: Ground surface elevation according to the Sep-11 LiDAR survey.

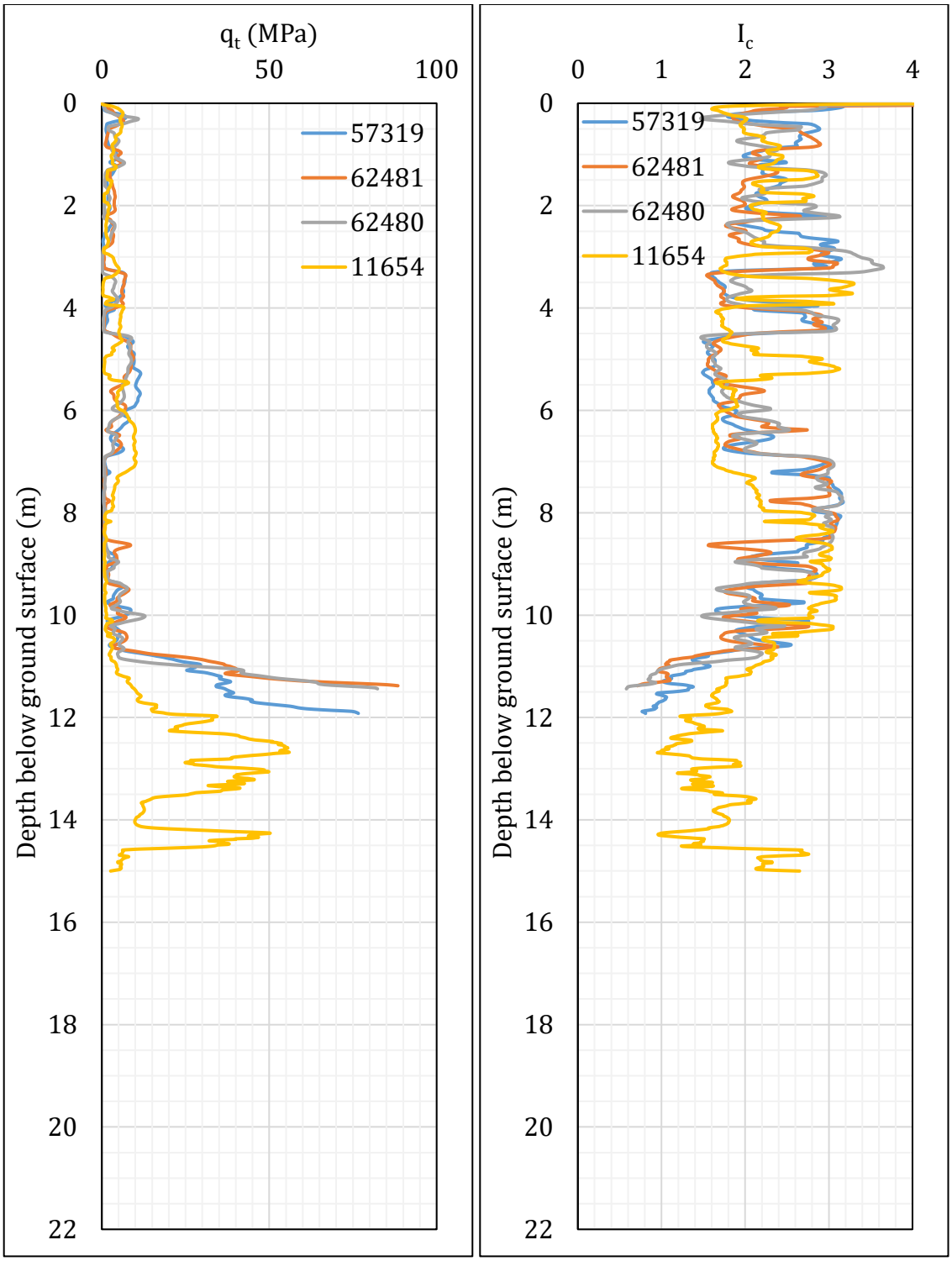

Figure 42: q_t and I_c profiles.

Note 5: The selection of CPTs for the area considered for settlement assessment (Figure 1) is based on the proximity of the CPTs to the considered areas. In accordance with that, the following table shows CPTs that were used for the volumetric settlement analysis in *Cliq v.3.0.3.2*, a CPT soil liquefaction software developed by GeoLogismiki. (The average volumetric settlements were reported in Table 8.)

Table 12: CPT profiles used in volumetric settlement analysis for Patch A selected for settlement assessment.

CPT ID No.	10-m buffer	20-m buffer	50-m buffer
57319 (56884)	✓	✓	✓
62481 (56886)	✓	✓	✓
62480 (56885)		✓	✓
116654 (127542)			✓

Notes: CPT 11654 was used to compute the volumetric settlement for a depth range from ~11.5-15 m for CPTs 57319, 62481, and 62480; It was assumed that below 15 m, the volumetric settlement was negligible; CPT 116654 is ~90 m to the SE from the center of the site, within the sports field.

Table 13: CPT-based results.

		CPT ID					
EQ Event	Parameter	57319	62481	62480	116654	$\Delta_{CPT\ 57319}$	$\Delta_{CPT\ 62481/62480}$
Sep-10	S_{V1D} (mm)	50	69	68	100	8	13
	LSN	7	10	10	16	1	1
	LPI	2	3	3	4	0	0
	LPI_{ish}	1	1	0	1	--	--
	$D_{FS<1}$ (m)	6.42	5.56	5.50	4.04	--	--
Feb-11	S_{V1D} (mm)	79	112	115	158	14	21
	LSN	13	20	21	28	1	2
	LPI	7	11	11	15	1	1
	LPI_{ish}	1	1	1	5	--	--
	$D_{FS<1}$ (m)	2.32	2.32	2.32	2.31	--	--
Jun-11	S_{V1D} (mm)	16	19	17	25	0	1
	LSN	2	2	2	4	0	0
	LPI	0	0	0	0	0	0
	LPI_{ish}	0	0	0	0	--	--
	$D_{FS<1}$ (m)	undet.	undet.	undet.	10.66	--	--
Dec-11	S_{V1D} (mm)	9	13	11	16	0	0
	LSN	1	2	2	2	0	0
	LPI	0	0	0	0	0	0
	LPI_{ish}	0	0	0	0	--	--
	$D_{FS<1}$ (m)	undet.	undet.	undet.	undet.	--	--

Notes: $D_{FS<1}$ = Depth to the first liquefiable layer ($FS_L<1$) that is at least 200-mm thick, as determined by the Boulanger and Idriss (2016) liquefaction-triggering procedure (P_L=50%, C_{FC}=0.13, and $I_{c,cutoff}$ =2.6), and exported from *Cliq v.3.0.3.2*; undet. = the specified soil layer was not detected; $\Delta_{CPT\ 57319}$ and $\Delta_{CPT\ 62481/62480}$ indicate the amount of SV1D, LSN, and LPI added to CPTs 57319 and 62481/62480, respectively, due to the shallow penetration depths.

Note 6: Based on the borehole log (BH 57220, Figure 1), the groundwater table is at a depth of 1.6 m below the ground surface. The soil profile consists of (1) organic silty, OL, topsoil to a depth of 0.9 m, (2) silt, ML, to a depth of 1.95 m, (3) silty fine sand, SM, to a depth of 2.20 m, (4) silt, ML, to a depth of 3.15 m, (5) fine to medium sand, SP, to a depth of 3.95 m, (6) silt, ML, with some organics to a depth of 4.6 m, (7) sandy silt, ML, to a depth of 5.4 m, (8) fine to medium sand, SP, to a depth of 5.65 m, (9) silty sand, SM, to a depth of 6.30 m, (10) silt, ML, with trace organics to a depth of 10.15 m, (11) silty sand, SM, to a depth of 10.4 m, (12) silt, ML, to a depth of 10.9 m, (13) sandy fine to coarse gravel, GW, to a depth of 12.4 m, (14) fine to medium sand, SP, to a depth of 12.8 m, (15) sandy fine to coarse gravel, GW, to a depth of 15.65 m (the end of the borehole). All soil layers, except the topsoil, are the Yaldhurst members of the Springston formation. Based on the nearby borehole logs, it is assumed that the GW layer continues to a depth of 20 m.